# CHAPTER 1

# PHYSICS OF MAGNETISM

## 1.1 INTRODUCTION

The aim of this book is to characterize the magnetization that results in a material when a magnetic field is applied. This magnetization can vary spatially because of the geometry of the applied field. The models presented in this book will compute this variation accurately, provided the scale is not too small. In the case of particulate media, the computation cells must be large enough to encompass a sufficient number of basic magnetic entities to ensure that the deviation from the mean number of particles is a small fraction of the number of particles in that cell. In the case of continuous media, the computation cells must be large enough to encompass many inclusions. The study of magnetization on a smaller scale, known as *micromagnetics*, is beyond the scope of this book. Nevertheless, we will see that it is possible to have computation cells as small as the order of micrometers.

This book presents a study of magnetic hysteresis based on physical principles, rather than simply on the mathematical curve-fitting of observed data. It is hoped that the use of this method will permit the description of the observed data with fewer parameters for the same accuracy, and also perhaps that some physical insight into the processes involved will be obtained. This chapter reviews the physics underlying the magnetic processes that exhibit hysteresis only in sufficient detail to summarize the theory behind hysteresis modeling; it is not intended as an introduction to magnetic phenomena.

This chapter's discussion begins at the atomic level, where the behavior of the magnetization is governed by quantum mechanics. This analysis will result in a methodology for computing magnetization patterns called micromagnetism. For a more detailed discussion of the physics involved, the reader is referred to the excellent books by Morrish [1] and Chikazumi [2].

Since micromagnetic problems involve hysteresis, there are many possible solutions for a given applied field. The particular solution that is appropriate depends on the history of the magnetizing process. We view the magnetizing process of hysteretic media as a many-body problem with hysteresis. In this chapter, we start by reviewing some physical principles of magnetic material behavior as a basis for developing models for behavior. Special techniques are devised in future chapters to handle this problem mathematically. The Preisach and Preisach-type models, introduced in the next chapter, form the basic framework for this mathematics. The discussion presented relies on physical principles, and we will not discuss the derived equations with mathematical rigor. There are excellent mathematical books addressing this subject, including those by Visintin [3] and by Brokate and Sprekels [4]. In subsequent chapters, when we modify the Preisach model so that it can describe accurately phenomena observed in magnetic materials, we will see all these physical insights and techniques.

## 1.2 DIAMAGNETISM AND PARAMAGNETISM

Both diamagnetic and paramagnetic materials have very weak magnetic properties at room temperature; neither kind displays hysteresis. Diamagnetism occurs in materials consisting of atoms with no net magnetic moment. The application of a magnetic field induces a moment in the atom that, by Lenz's law, opposes the applied field. This leads to a relative permeability for the medium that is slightly less than unity.

Paramagnetic materials, on the other hand, have a relative permeability that is slightly greater than 1. They may be in any material phase, and they consist of molecules that have a magnetic moment whose magnitude is constant. In the presence of an applied field, such a moment will experience a torque tending to align it with the field. At a temperature of absolute zero, the electrons or atoms with a magnetic moment in assembly would align themselves with the magnetic field. This would produce a net magnetization, or magnetic moment per unit volume, equal to the product of their moment and their density. This is the maximum magnetization that can be achieved with this electron concentration, and thus it will be called the *saturation magnetization M<sub>S</sub>*. Atoms possess a magnetic moment that is an integer number of Bohr magnetons. The magnetic moment of an electron,  $m_{\rm B}$ , is one Bohr magneton, which in SI units is  $0.9274 \times 10^{-23} \, {\rm A-m^2}$ . We note that the permeability of free space  $\mu_0$ , and Boltzmann's constant, k, are in SI units  $4\pi \times 10^{-7}$  and  $1.3803 \times 10^{-23} \, {\rm J/mole-deg}$ , respectively.

Paramagnetic behavior occurs when these atoms form a reasonably dilute electron gas. At temperatures above absolute zero, for normal applied field

strengths, thermal agitation will prevent them from completely aligning with that field. Let us define B as the applied magnetic flux density, and T as the absolute temperature. Then if we define the *Langevin function* by

$$L(\xi) = \coth \xi - \frac{1}{\xi}, \tag{1.1}$$

then the magnetization is proportional to the Langevin function, so that

$$M = M_S L(\xi), \tag{1.2}$$

where

$$\xi = \frac{\mu_0 g J m_{\rm B} H}{kT} = \frac{\mu_0 m H}{kT}. \tag{1.3}$$

Here the moment of the atom, m, is the product of g, the gyromagnetic ratio, J the angular momentum quantum number, and  $m_B$  the Bohr magneton. It can be shown that the distribution of magnetic moments obeys Maxwell-Boltzmann statistics [5]. Figure 1.1 shows a plot of the Langevin function and its derivative. It is seen that for small  $\xi$  the function is linear with slope 1/3 and saturates at unity for large  $\xi$ .

The susceptibility of the gas, the derivative of the magnetization with respect to the applied field, is given by

$$\chi(H) = \frac{dM}{dH} = \frac{M_S \xi}{H} \left[ \frac{1}{\xi^2} - \operatorname{csch}^2(\xi) \right]. \tag{1.4}$$

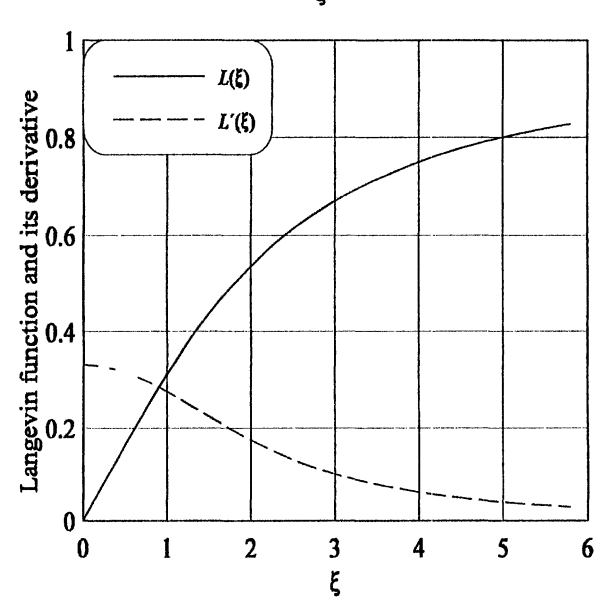


Figure 1.1 Langevin function (solid line) and its derivative (dashed line).

For small  $\xi$ , the quantity in brackets approaches 1/3. Thus, when the applied fields are small, the susceptibility,  $\chi_0$  is given by

$$\chi_0 = \frac{M_S \xi}{3H} = \frac{\mu_0 m M_S}{3kT}.$$
 (1.5)

The small field susceptibility as a function of temperature is shown in Fig. 1.2.

At room temperature, the argument of the Langevin function is very small, and this effect is very weak; that is, the misalignment due to thermal motions is much greater than the effect of the applied field. Thus, this effect is not significant in the description of hysteresis; however, when discussing ferromagnetic materials, we will see that their behaviors above the Curie temperature are similar, except that the susceptibility diverges at the Curie temperature rather than at absolute zero.

The previous analysis did not include quantization effects. Since the magnetic moment can vary only in integer multiples, the Langevin function must be replaced by the Brillouin function,  $B_j(\xi)$ . The *Brillouin function* is defined by

$$B_J(\xi) = \frac{2J+1}{2J} \coth \frac{2J+1}{2J} \xi - \frac{1}{2J} \coth \frac{\xi}{2J}.$$
 (1.6)

Thus, the magnetization M(T) at temperature T, is given by

$$M(T) = Nm_{\rm B}gJB_J(\xi), \qquad (1.7)$$

where, N is the number of atoms per unit volume, g is 0.5 for the electron, and J, an integer, is the angular momentum quantum number. The Brillouin function is zero if  $\xi$  is zero, and approaches one if  $\xi$  becomes large, as seen in Fig. 1.3. Therefore, from (1.7) we have

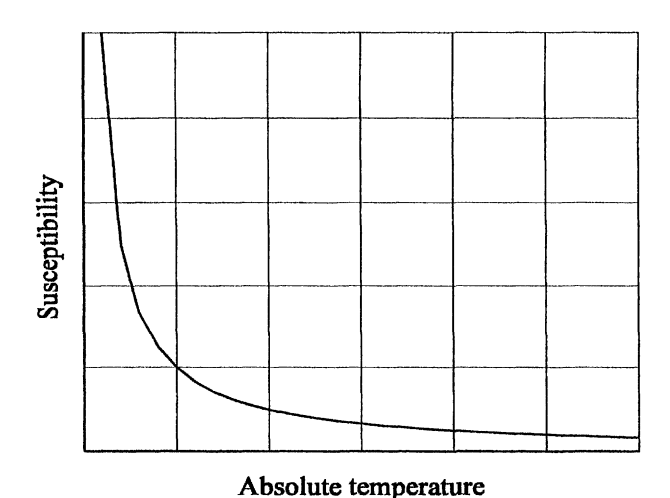


Figure 1.2 Paramagnetic susceptibility as a function of temperature.

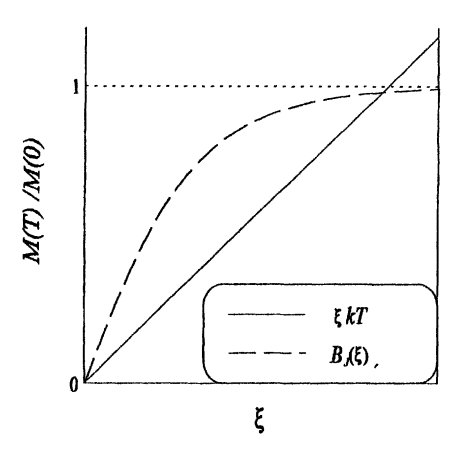


Figure 1.3 Plot of  $B_J(\xi)$  and the linear function,  $\xi kT$  as a function of  $\xi$  for J=1.

$$M(0) = Nm_{\rm B}gJ, \tag{1.8}$$

and so

$$\frac{M(T)}{M(0)} = B_j(\xi). \tag{1.9}$$

For small  $\xi$ , the Brillouin function is given approximately by

$$B_{J}(\xi) \approx \frac{J+1}{3J}\xi. \tag{1.10}$$

# 1.3 FERRO-, ANTIFERRO- AND FERRIMAGNETIC MATERIALS

In accordance with the Pauli exclusion principle, electrons obey Fermi-Dirac statistics; that is, only one electron can occupy a discrete quantum state at a time. When atoms are placed close together as they are in a crystal, the electron wave functions of adjacent atoms may overlap. Here, it is found that given a certain direction of magnetization for one atom, the energy of the second atom is higher for one direction of magnetization than the other. This difference in energy between the two states is called *exchange energy*. Furthermore, when the parallel magnetization is the lower energy state, the exchange is said to be *ferromagnetic*, but when the antiparallel magnetization is the lower energy state, the exchange is said to be *antiferromagnetic*. In ferromagnetic materials, this energy is very large and causes adjacent atoms to be magnetized in essentially the same direction at normal temperatures. Pure metal crystals of only three elements, iron, nickel, and cobalt, are ferromagnetic.

Since the electron wave functions are very localized, the overlap of wave functions between adjacent atoms decreases very quickly to zero as a function of the distance between them. Thus, exchange energy is usually limited to nearest neighbors. Sometimes the intervening atoms in a compound can act as a medium so that more distant atoms can be exchange coupled. Here, the resulting exchange is called *superexchange*. This, can also be either ferromagnetic or antiferromagnetic. Thus, compounds such as chromium dioxide can also be ferromagnetic.

The effect of exchange energy can be accounted for by an equivalent exchange field. Thus, the field, H, that an atomic moment experiences is given by

$$H = H_A + N_W M, \tag{1.11}$$

where  $H_A$  is the applied field,  $N_W$  is the molecular field constant, and  $N_W M$  is the exchange field. Substituting this into (1.3), one sees that  $\xi$  is now given by The remanence is obtained by setting H equal to zero in this equation and solving

$$\xi = \frac{\mu_0 g J m_B [H + N_W M(T)]}{kT}. \tag{1.12}$$

for M(T). Thus,

$$M(T) = \frac{\xi kT}{\mu_0 g J m_{\rm p} N_{\rm w}},\tag{1.13}$$

and we can use (1.8) to write this as follows:

$$\frac{M(T)}{M(0)} = \frac{\xi kT}{\mu_0 g^2 m_B^2 J^2 N N_W} = \xi kT. \tag{1.14}$$

Since this must also be equal to the Brillouin function, we can obtain a graphical solution by plotting the two functions on the same graph, as illustrated in Fig. 1.3. For low temperatures, the slope of (1.14) is very small, so the intersection occurs at large values of  $\xi$ , and thus normalized magnetization approaches unity. As the temperature increases, the slope also increases, and thus, the magnetization decreases.

At the Curie temperature,  $\Theta$ , the slopes of (1.14) and that of the Brillouin function are equal. This intersection occurs at a point where both  $\xi$  and the magnetization are zero. The Curie temperature can be computed, since from (1.10), the slope of the Brillouin function is given by

$$\frac{dB_{J}(\xi)}{d\xi}\bigg|_{\xi=0} = \frac{J+1}{3J} = k\Theta. \tag{1.15}$$

Thus, the Curie temperature is

$$\Theta = \frac{\mu_0 g^2 m_B^2 J(J+1) N N_W}{3k}.$$
 (1.16)

Becker and Döring [6] computed the saturation magnetization as a function of temperature and the total angular momentum. A comparison with measured values for iron and nickel, as shown in Fig. 1.4, appears to be a good fit with theory if J is taken to be either 0.5 or 1.

Above the Curie temperature, the material acts as a paramagnetic medium with the susceptibility diverging at a temperature called the *Curie–Weiss temperature* rather than at absolute zero degrees. The latter temperature is close to the Curie temperature for most materials. This type of behavior occurs regardless of whether the material is single crystal or consists of many particles or grains that are larger than a certain critical size. However, for small particles or grains another effect occurs. We will show in Section 1.6 that if these grains are sufficiently small, they may have only two stable states separated by an energy barrier. It is then possible that at a temperature smaller than the Curie temperature, called the *blocking temperature*, the thermodynamic energy *kT* will become comparable to the barrier energy. In that case, the particles or grains can spontaneously reverse and the material no longer will appear to be ferromagnetic. Above the blocking temperature, it behaves like a paramagnetic material with grains that have moments much larger than the spin of a single electron. This type of behavior is called

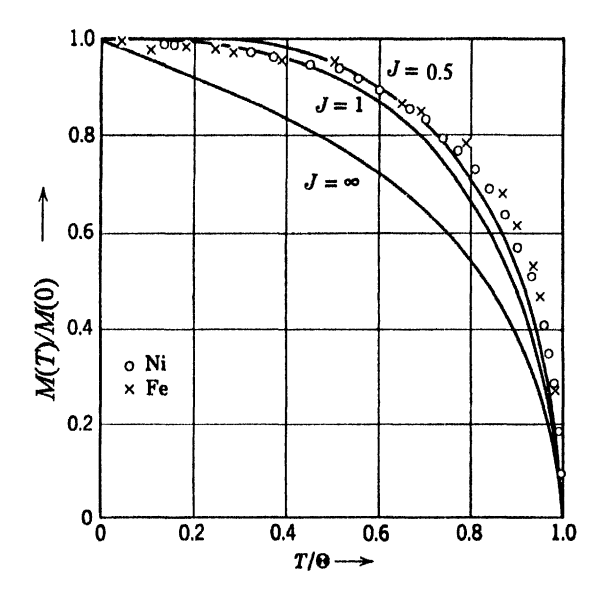


Figure 1.4 Temperature variation of saturation magnetization for atoms with different total angular momentum. [After Becker and Döring, 1939.]

superparamagnetism. As the temperature is raised from below, the material appears to lose its remanence and has a sudden large increase in its susceptibility. For a medium with a distribution of grain sizes, there is a distribution in energy barriers so that the blocking temperature is diffuse.

If the exchange energy is negative, it is convenient to think of the material as composed of two sublattices magnetized in the opposite directions. If the magnitude of the magnetization is the same for these two antiparallel sublattices, the net magnetization will be zero, and the material is said to be *antiferromagnetic* and appears to be nonmagnetic. On the other hand, if the magnitude differs, the material will have a net magnetization; such a material is said to be *ferrimagnetic*.

Ferrimagnetic materials usually have smaller saturation magnetization values than ferromagnetic materials, because the two sublattices have opposite magnetization. These materials are important, since they usually occur in ceramics that either are insulators or have very high resistivity. Such materials will support negligible eddy currents and so will be useful to very high frequencies.

The materials will be ferrimagnetic for all temperatures below a critical temperature, known as the *Néel temperature*. Above that temperature the materials also become *superparamagnetic*, similar to the way ferromagnetic materials behave above the Curie temperature. Since the two sublattices may have different temperature behavior, it is possible that at a given temperature the two moments may be equal but opposite in sign, as illustrated in Fig. 1.5. At this temperature, known as the *compensation temperature*, the two sublattices have equal magnetization so that the net magnetization is zero. This magnetization is the magnitude of the difference between the two sublattice magnetizations and will be positive, since above or below the compensation temperature, the material will become magnetized in the direction of an applied field.

The compensation temperature occurs above, below, or at room temperature, depending on the elements in the crystal. Unlike the demagnetized state above the Curie temperature, this state "remembers" its magnetic state, and changing its temperature from the compensation temperature reproduces the previous magnetic state. This property is useful in magneto-optical disks to render the stored information impervious to stray fields. This is done by choosing a compensation temperature that is close to the storage temperature. For practical devices the storage temperature is usually room temperature.

#### 1.4 MICROMAGNETISM

In this section we assume that the temperature is fixed so that material parameters, such as saturation magnetization, may be regarded as constants. We then compute the equilibrium magnetization patterns in a ferromagnetic medium. The dynamics of magnetization are discussed in later sections. Thus, we choose the magnetization variation that minimizes the total energy. This total energy is the sum of the exchange energy, the magnetocrystalline anisotropy energy, and the Zeeman energy.

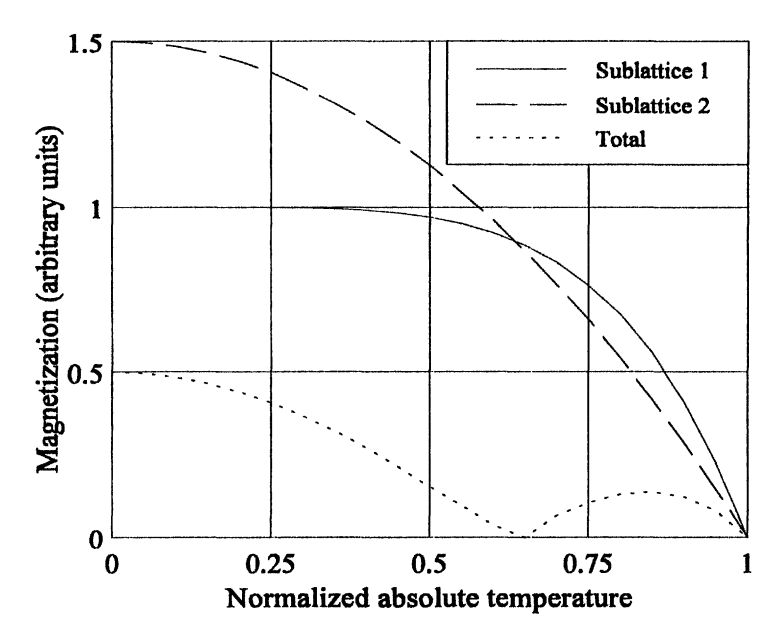


**Figure 1.5** A ferrimagnetic material with a compensation temperature of approximately 65% of its Néel temperature.

The exchange energy, the source of the ferromagnetism, is given by

$$W_{\rm ex} = \sum_{\rm n.n.} J \mathbf{S_i} \cdot \mathbf{S_j}, \tag{1.17}$$

where n.n. denotes that the sum is carried out over all pairs of nearest neighbors, J is the exchange integral, and S is the spin vector. Since the wave functions are not isotropic, the exchange energy is not only a function of the difference in orientation of adjacent spins, but is also a function of the direction of the spins. Since a spin interacts with several nearest neighbors, the orientation energy depends upon the crystal structure. This variation in the exchange energy with spin orientation is called the *magnetocrystalline anisotropy energy*. We take it into account by adding an anisotropy energy density term to (1.17). For cubic crystals, the simplest form of this is given by

$$W_{\text{cubic}} = K(\alpha_x \alpha_y + \alpha_y \alpha_z + \alpha_z \alpha_x), \qquad (1.18)$$

where the  $\alpha$ 's are the direction cosines with respect to the crystalline axes, and K is the anisotropy constant. If K is positive, the minimum anisotropy energy density occurs along each of the three axes of the crystal. On the other hand, if K is negative, the minimum anisotropy energy density occurs along the four axes that make equal angles with respect to the three crystal axes. Higher order terms may be added to this in certain cases.

Another type of anisotropy energy density that commonly occurs is the uniaxial anisotropy energy density. This is given by

$$W_{\rm u} = K_{\rm u} \sin^2 \theta \,, \tag{1.19}$$

where  $K_u$  is the uniaxial anisotropy constant,  $\theta$  is the angle the magnetization makes with respect to the z axis, and z is the easy axis if  $K_u$  is positive. If  $K_u$  is negative, then z is the hard axis, and the plane perpendicular to the z axis is the easy plane. We will denote the anisotropy energy density by  $W_{anis}$  whether it is cubic or uniaxial.

For the present, we will consider only one additional energy term, the *Zeeman energy*, which is the energy that a magnetic dipole **m** has due to a magnetic field. This energy is given by

$$W_{\text{Zeeman}} = -\mathbf{m} \cdot \mathbf{B}, \tag{1.20}$$

where **B** is the total magnetic field, which is the sum of the external applied field and the demagnetizing field of the body. We will decompose this term into the sum of the applied field energy and the demagnetizing energy. The energy of a magnetized body in an external field is given by

$$W_{\rm H} = \int_{V} \mathbf{B} \cdot \mathbf{H} \ dV. \tag{1.21}$$

Since B is  $\mu_0(\mathbf{H} + \mathbf{M})$ , and since  $M^2$  is constant, by choosing a different reference energy, this reduces to

$$W_{\rm H} = \mu_0 \int_V \mathbf{M} \cdot \mathbf{H} \, dV, \tag{1.22}$$

where  $\mathbf{H}$  is that applied field and V is the volume of the material. Similarly, the self-demagnetizing energy is given by

$$= \frac{\mu_0}{2} \int_V \mathbf{M} \cdot \mathbf{H}_D dV, \qquad (1.23)$$

where  $H_D$  is the demagnetizing field.

Thus, the total energy of the body is given by

$$W = W_{\rm ex} + W_{\rm anis} + W_{\rm D} + W_{\rm H}. \tag{1.24}$$

The magnetization pattern is then determined by adjusting the orientation of the magnetization at each point in the material to minimize the total energy. In principle we could find the orientation of the magnetization of each atom in the medium, but unless the object is very small, this would involve too many computations. Instead, in micromagnetism, we will define a continuous function whose value at each atomic site is the magnetization of that atom.

Micromagnetism is the study of magnetization patterns in a material at a level of resolution at which the discrete atomic structure is blended into a continuum, but the details are still visible. Thus, the orientation of the magnetization in the medium is obtained from a continuous function defined over the medium. Summations are replaced by integrations, and differences by derivatives. In particular, if  $\mathbf{r}$  is the position of an atom and  $\mathbf{a}$  is the relative position of a neighbor, the exchange energy density between them is given by

$$w_{\text{ex}} = -\lim_{a \to 0} \frac{2J\mathbf{s}(\mathbf{r}) \cdot \mathbf{s}(\mathbf{r} + \mathbf{a})}{a^3}.$$
 (1.25)

Since the magnetization and the spin vector are in the same direction, we can replace s by  $sM/M_s$ , where s is the magnitude of the spin vector and  $M_s$  is the magnitude of M. Then, if we expand  $S(\mathbf{r}+\mathbf{a})$  in a Taylor series, we get

$$\mathbf{s}(\mathbf{r}+a\mathbf{1}_{x}) = \frac{s}{M_{s}} \left[ \mathbf{M}(\mathbf{r}) + a \frac{\partial \mathbf{M}(\mathbf{r})}{\partial x} + \frac{a^{2}}{2} \frac{\partial^{2} \mathbf{M}(\mathbf{r})}{\partial x^{2}} + \cdots \right], \tag{1.26}$$

where a is the distance to the nearest neighbor atom in the x direction and  $\mathbf{1}_x$  is a unit vector in the x direction. Then

$$\mathbf{s}(\mathbf{r})\cdot\mathbf{s}(\mathbf{r}+a\mathbf{1}_{x}) = \frac{s^{2}}{M_{s}^{2}} \left[ 1 + a\mathbf{M}(\mathbf{r}) \cdot \frac{\partial \mathbf{M}(\mathbf{r})}{\partial x} + \frac{a^{2}}{2}\mathbf{M}(\mathbf{r}) \cdot \frac{\partial^{2}\mathbf{M}(\mathbf{r})}{\partial x^{2}} + \cdots \right]. \quad (1.27)$$

The first term in the Taylor series is a constant and can be omitted by choosing a different energy reference. Since

$$\mathbf{M} \cdot \frac{\partial \mathbf{M}}{\partial x} = \frac{1}{2} \frac{\partial M^2}{\partial x},\tag{1.28}$$

and since  $M^2$  is a constant, the second term in (1.27) is zero. If we sum the terms in the y and z directions as well, then for a simple cubic crystal, the total exchange energy becomes

$$\sigma W_{ex} = -\frac{A}{M_s^2} \int_{V} \mathbf{M} \cdot \left( \frac{\partial^2 \mathbf{M}}{\partial x^2} + \frac{\partial^2 \mathbf{M}}{\partial y^2} + \frac{\partial^2 \mathbf{M}}{\partial z^2} \right) dV$$

$$= -\frac{A}{M_s^2} \int_{V} \mathbf{M} \cdot \nabla^2 \mathbf{M} dV,$$
(1.29)

where

$$A = \frac{Js^2}{a}. ag{1.30}$$

Because of the additional atoms in a unit cell, for a body-centered cubic lattice the exchange constant A is twice the value of a simple cubic lattice, and for a face-centered cubic lattice it is four times the value of a simple cubic lattice.

It is noted that (1.29) is approximate in two respects. First, the Taylor series is truncated. Thus, the change in magnetization between adjacent atoms is assumed to be small to allow the series to converge rapidly. This assumption is usually valid. The second approximation is more subtle in that we are approximating a discrete function by a continuous function. Since  $M^2$  is constant, the second derivative of the magnetization diverges at the center of a vortex. Thus, (1.29) would calculate an infinite energy, although  $Js(\mathbf{r}) \cdot s(\mathbf{r} + a\mathbf{1}_{\mathbf{x}})$  remains finite at the center of the vortex.

The equilibrium magnetization in a medium is obtained by varying the direction of the magnetization so as to minimize the total energy. This can be done by directly minimizing the energy or by solving the Euler-Lagrange partial differential equation corresponding to this variational problem. The resulting magnetization pattern is referred to as the *micromagnetic solution*. This calculation must be performed numerically, except for a few cases, two of which are discussed in the next two sections. This introduces an additional discretization error that calculates a finite energy at the center of the vortex. This energy is incorrect unless the discretization distance is the same as the size of the magnetic unit cell.

If one is interested in the details of the magnetization change when the applied field changes, the dynamics of the process must be introduced. Two such effects — eddy currents, in materials with finite conductivity, and gyromagnetism — are discussed later.

## 1.5 DOMAINS AND DOMAIN WALLS

An equilibrium solution to the micromagnetic problem in an infinite medium is uniform magnetization along an easy axis. Then, both the exchange energy and the anisotropy energy are zero. Such a region of uniform magnetization is called a *domain*. In an infinite medium that is not uniformly magnetized, we will now see that the equilibrium solution is the division of the medium into many domains that are separated by domain walls that have essentially a finite thickness. Domain walls of many types are possible, but in this section we discuss only the two simplest types: the *Bloch wall* and the *Néel wall*. Furthermore, domain walls are classified by the difference in the orientations of the domains that they separate, expressed in degrees. For brevity, we limit ourselves to 180° walls.

We will consider a domain wall whose center is at x = 0, which divides a domain that is magnetized in the y direction as x goes to infinity and that is magnetized in the -y direction as x goes to minus infinity. As one goes from one domain to the other, if the magnetization rotates about the x axis, it remains in the plane of the wall, and the wall is said to be a *Bloch wall*. On the other hand, if the magnetization rotates about the x axis, the wall is said to be a *Néel wall*.

# 1.5.1 Bloch Walls

Let us consider a Bloch wall that lies in the yz plane and that separates two domains: one magnetized in the y direction and the other magnetized in the -y direction. If the domain magnetized in the y direction lies in the region of positive x, and the domain magnetized in the -y direction lies in the region of negative x, then the magnetization can be written as

$$M(x) = M_S \{\cos[\theta(x)]\mathbf{1}_y + \sin[\theta(x)]\mathbf{1}_z\},$$
 (1.31)

with the boundary conditions  $\theta(-\infty) = 0$  and  $\theta(\infty) = \pi$ . That is, the magnetization is in the z direction for large negative values of x and in the -z direction for large positive values of x. Differentiating twice with respect to x, we have

$$\frac{\partial^2 \mathbf{M}}{\partial x^2} = -\mathbf{M} \left( \frac{\partial \mathbf{\theta}}{\partial x} \right)^2, \tag{1.32}$$

so that

$$\mathbf{M} \cdot \frac{\partial^2 \mathbf{M}}{\partial x^2} = -M_S^2 \left(\frac{d\theta}{dx}\right)^2. \tag{1.33}$$

If there is no applied field, and since there is no demagnetizing field, the Zeeman energy is zero. Summing the remaining energies, the anisotropy energy and exchange energy, from (1.29), the energy in a domain wall per unit area is as follows:

$$W = \int_{-\infty}^{\infty} \left[ A \left( \frac{\partial \theta}{\partial x} \right)^2 + g[\theta(x)] \right] dx, \qquad (1.34)$$

where  $g[\theta(x)]$  is the volume density anisotropy energy function.

We obtain the domain wall shape by finding the  $\theta(x)$ , which minimizes this integral subject to the constraints that  $\theta(-\infty) = 0$  and  $\theta(\infty) = \pi$ . This minimum is found, using the calculus of variations, by solving the corresponding Lagrange differential equation corresponding to the minimization of this integral. In this case, this is given by

$$\frac{dg(\theta)}{d\theta} - 2A\left(\frac{d^2\theta}{dx^2}\right) = 0. {(1.35)}$$

If we integrate this from 0 to  $\theta$ , since g(0) is zero and since  $d\theta/dx|_{x=-\infty}$  is zero, we obtain

$$g(\theta) = 2A \int_0^\infty \frac{d^2\theta}{dx^2} d\theta = A \int_{-\infty}^x \frac{d}{dx} \left(\frac{d\theta}{dx}\right)^2 dx = A \left(\frac{d\theta}{dx}\right)^2, \quad (1.36)$$

or

$$x = \int_0^{\theta} \sqrt{\frac{A}{g(\theta)}} d\theta. \tag{1.37}$$

For crystals with uniaxial anisotropy, from (1.19),

$$g(\theta) = K_{\rm u} \cos^2 \theta \,. \tag{1.38}$$

Then

$$x = \sqrt{\frac{A}{K_{\rm u}}} \int_0^{\theta} \frac{d\theta}{\sin\theta} = \frac{l_{\rm w}}{\pi} \ln\left(\tan\frac{\theta}{2}\right), \tag{1.39}$$

where  $l_w$  is the classical wall width given by

$$l_{\rm w} = \pi \sqrt{A/K_{\rm u}}.\tag{1.40}$$

For iron, this is approximately 42 nm, or roughly 150 atoms wide. Solving for  $\theta$ , one gets

$$\theta = \tan^{-1} \left( \exp \frac{\pi x}{l_w} \right) = \operatorname{gd} \left( \frac{\pi x}{l_w} \right) - \frac{\pi}{2}, \tag{1.41}$$

where gd, defined by this equation, is called the *Gudermannian*. Figure 1.6 plots  $\theta$  as a function of x. It is seen that more than half of the rotation in angle takes place between  $\pm l_w$ . In fact, in the equal angle approximation all the rotation takes place between  $\pm l_w$ . Since for many magnetic materials  $l_w$  is the order of 0.1  $\mu$ m, the domain wall is very localized. Substituting (1.36) into (1.34), we see that the total energy density per unit wall area is given by

$$w = 2 \int_{-\pi/2}^{\pi/2} g(\theta) \frac{dx}{d\theta} d\theta = 2 \int_{-\pi/2}^{\pi/2} \sqrt{Ag(\theta)} d\theta. \qquad (1.42)$$

Thus, for uniaxial materials, this becomes

$$w = 2 \int_{-\pi/2}^{\pi/2} \sqrt{AK_u \sin^2\theta} \, d\theta = 4\sqrt{AK_u}. \tag{1.43}$$

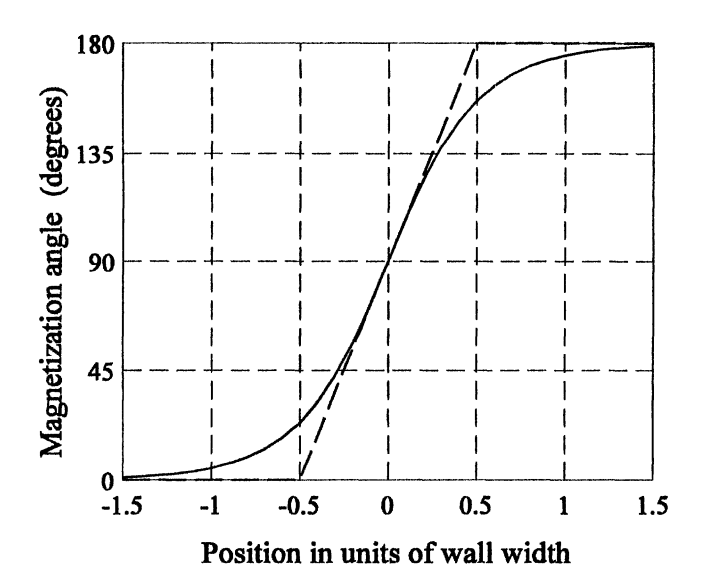


Figure 1.6 Variation of the magnetization angle for a Bloch wall: Dashed line indicates the equal angle approximation to the angle variation.

#### 1.5.2 Néel Walls

For an infinite Néel wall, the magnetization is given by

$$\mathbf{M} = M_{S} \left[ \cos \theta(x) \mathbf{1}_{x} + \sin \theta(x) \mathbf{1}_{z} \right], \tag{1.44}$$

where  $\theta$  goes from 0 to  $\pi$  as x goes from  $-\infty$  to  $\infty$ . The only difference between this and the Bloch wall is that the magnetization now turns so that when x is zero it points from one domain to the other. In this case, the divergence of  $\mathbf{M}$  is no longer zero, and there is a Zeeman term in the total energy. Since the divergence of  $\mathbf{B}$  is zero, the divergence of  $\mathbf{M}$  is the negative of the divergence  $\mathbf{H}$ . In particular,

$$\operatorname{div} \mathbf{M} = \frac{\partial M_x}{\partial x} = M_s \cos \theta(x) \frac{d\theta}{dx} = -\operatorname{div} \mathbf{H}. \tag{1.45}$$

Since **H** has only an x component, when we integrate this equation and use the boundary conditions that  $\mathbf{H}(-\infty) = \mathbf{H}(\infty) = 0$ , we are led to the conclusion that  $H_x = -M_s$ . From (1.23), the demagnetizing energy of the moments in this field is given by

$$W_D = -\frac{\mu_0 H_x M_S}{2} = \frac{\mu_0 M_x^2}{2} = \frac{\mu_0 M_S^2}{2} \cos^2 \theta(x). \tag{1.46}$$

Comparison with (1.38) shows that this has the same variation as the uniaxial anisotropy energy. Thus, a Néel wall has the same shape as a Bloch wall whose

anisotropy energy is given by  $K_u + \mu M_s^2$ . Since the wall energy is proportional to the square root of  $K_u$ , it is seen that the Néel wall will have greater energy than a Bloch wall. Thus, in infinite media, Bloch walls are energetically preferable to Néel walls. Furthermore, since the wall width is inversely proportional to the square-root of  $K_u$ , it is seen that the Néel wall will be thinner than a Bloch wall.

We have just discussed domain walls in infinite media. In finite media, the walls will interact with boundaries. Thus, in thin films, 180° walls between domains magnetized in the plane of the film tend to be Néel walls, to minimize demagnetizing fields. Furthermore, at the junction of two walls of opposite rotation, complex wall structures can form, such as cross-tie walls. This subject is beyond the scope of this chapter.

# 1.5.3 Coercivity of a Domain Wall

In the continuous micromagnetic case, the energy is not a function of the position of the domain wall. Thus the slightest applied field will raise the energy of the domain on one side of the wall with respect to the other, and there will be nothing to impede its motion, thus predicting zero coercivity. In a real crystal, the magnetization is not continuous because there are preferred positions of the domain wall, so there is a very small coercivity. The sources of coercivity in a real material are the imperfections in the crystal structure. We will briefly discuss imperfections of two types: *inclusions* and *dislocations* in the crystal lattice.

Inclusions are small "holes" in the medium, usually formed by the entrapment of bits of foreign matter. The inclusions either are nonmagnetic or have a much smaller magnetization than their surroundings. Such an inclusion will have magnetic poles induced on its surface, which will repel an approaching domain wall, thus impeding its progress. The equilibrium position of this wall in the absence of an applied field will be between the inclusions. The absence of exchange and anisotropy energy in the inclusion implies that the domain wall will have lower energy when it is situated on the inclusion also impeding its progress.

When a field is applied to a material with inclusions, the wall will bend in a direction that increases the volume of the domain that is closer to being parallel to the applied field. When the field is increased beyond a critical value, the domain will snap past that inclusion and become attached to another inclusion. We will denote the applied field behavior of the magnetization of the volume swept out by this motion as a *hysteron*. Even if it were possible to sweep that volume back, the field required to sweep the domain wall back generally would differ from the negative of the preceding field, which is now being restrained by different inclusions. Furthermore, these two fields are statistically independent of each other.

Dislocations in the crystal lattice also interact with domain walls. In some cases, the easy axes on the two sides of the dislocation may be aligned differently. This permits walls to be noninteger multiples of  $90^{\circ}$ . If the dislocations are sufficiently severe, the exchange interaction between atoms on the two sides of the

wall may become negligible and a domain wall might not be able to cross the boundary.

A hysteron can switch either by rotation of the magnetization in the domain, as discussed in the next section, or by wall motion. In the latter case, if there is a wall, it has to be translated past the inclusions. On the other hand, if the material had been saturated, so that all the domain walls were annihilated, a new wall would have to be nucleated. The nucleation of a reversed domain requires a much higher field than that required to move a wall past each inclusion. Thus, nucleation usually takes place only when there are no domain walls anywhere in the crystal. If one measures the hysteresis loop of a material by controlling the rate of change of magnetization to a very slow rate, the field required for the initial change in magnetization is found to be larger than that needed for subsequent changes in magnetization. The resulting loop is said to be reentrant. Such a loop is shown in Fig. 1.7. The random variation in width is due to the variation in coercivity from inclusion to inclusion.

# 1.6 THE STONER-WOHLFARTH MODEL

A magnetic medium consisting of tiny particles can have a much higher coercivity than a continuous medium with inclusions. A model to analyze this case by means of an ellipsoidal particle was proposed by Stoner and Wohlfarth [7], who used a theorem, shown by Maxwell, that the demagnetizing field of a uniformly magnetized ellipsoid is also uniform. Thus, it is possible to have an object in which the applied field, the demagnetizing field, and the magnetization are all uniform. This model is called the *coherent magnetization model*. Other magnetization modes are possible if the material is large enough, but for bodies whose largest dimension is smaller than the width of a domain wall, only the uniform magnetization mode

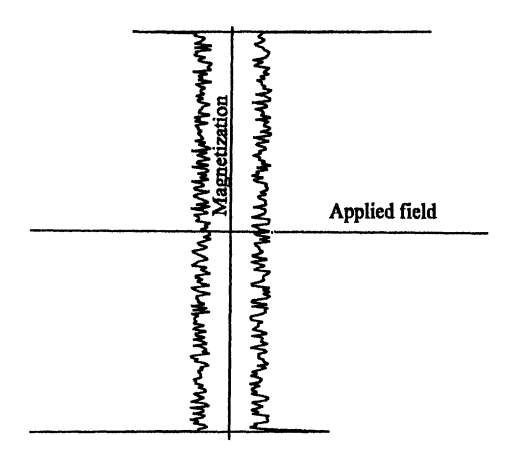


Figure 1.7 A typical reentrant hysteresis loop.

is possible. In such cases, we say that the particle is a *single domain particle*. Of course if the particle is too small, thermal energy might be sufficient to demagnetize it, and the particle would become *superparamagnetic*. That is, it would behave like a paramagnetic particle with a very large moment.

The Stoner-Wohlfarth model assumes that the particle is an ellipsoid and that its long (easy) axis is aligned with its magnetocrystalline uniaxial easy axis. It is also assumed that as the magnetization rotates, its magnitude remains constant. Because we assume that the particle is single domain, that is, it is uniformly magnetized, its exchange energy is seen to be zero. As the magnetization of the particle is rotated, the demagnetizing field changes in magnitude, and thus the demagnetizing energy changes because the demagnetizing factors along the different axes of the particle differ. This energy is referred to as *shape anisotropy energy*. Then magnetization will be oriented in such a way that the total energy — the sum of the applied field energy, the demagnetizing energy, and the shape anisotropy energy — is minimized. The sum of the latter two energies will be referred to simply as the *anisotropy energy*.

We will assume that a field is applied horizontally to a particle whose long axis makes an angle  $\beta$  with it, as shown in Fig. 1.8. All angles are measured in the counterclockwise direction, so that  $\theta$ , the angle the magnetization makes with respect to the particle's long axis, as pictured, is negative. We will presently see that if the applied field is zero, the magnetization will lie along the easy axis of the particle; however, it could be oriented either way along that axis. Thus, the anisotropy energy will be doubly periodic as the magnetization rotates. We will also see that the applied field energy is unidirectional and thus is singly periodic.

Maxwell showed that for a uniformly magnetized general ellipsoid, the demagnetizing field is also uniform, though not antiparallel to it. The demagnetizing field can be written as the product of the demagnetization tensor and the magnetization. The demagnetization tensor is diagonalized if the coordinate axes are chosen to be the principal axes of the ellipsoid. In that case, the diagonal elements are referred to as the demagnetizing factors, and the demagnetizing field

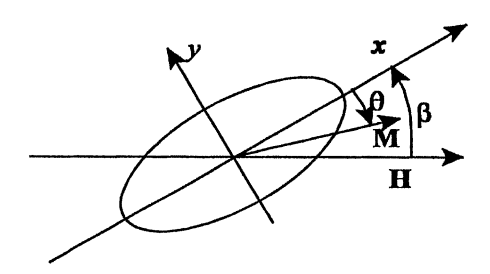


Figure 1.8 Stoner-Wohlfarth description of a spheroidal particle.

 $H_{\rm D}$  is given by

$$H_{\rm D} = D_{\rm x} M_{\rm x} 1_{\rm x} + D_{\rm v} M_{\rm v} 1_{\rm v} + D_{\rm z} M_{\rm z} 1_{\rm z}, \tag{1.47}$$

where  $D_x$ ,  $D_y$ ,  $D_z$  are the demagnetizing factors along the three principal axes of the ellipsoid. Maxwell also showed that

$$D_{x} + D_{y} + D_{z} = 1. {(1.48)}$$

For a spheroid, an ellipsoid of revolution, if the y and z are the two equal axes, then

$$D_{y} = D_{z} = \frac{1 - D_{x}}{2}. (1.49)$$

It is well known that for this spheroid

$$D_x = \frac{1}{\alpha^2 - 1} \left[ \frac{\alpha}{\sqrt{\alpha^2 - 1}} \ln \left( \alpha + \sqrt{\alpha^2 - 1} \right) - 1 \right], \quad \text{for } \alpha > 1, \tag{1.50}$$

and

$$D_{x} = \frac{1}{1-\alpha^{2}} \left[ 1 - \frac{\alpha}{\sqrt{1-\alpha^{2}}} \sin^{-1}\sqrt{1-\alpha^{2}} \right], \text{ for } \alpha < 1,$$
 (1.51)

where  $\alpha$  is the ratio of the length of the particle along the x axis to the length of the particle along other axes (see Bozorth [8]). It can be shown that as  $\alpha$  approaches one for both formulas, the demagnetization factor approaches 1/3, the value for a sphere. It can also be shown that when  $\alpha = 0$ , then  $D_x = 1$ , and for large  $\alpha$  (1.50) becomes

$$D_x = \frac{1}{\alpha^2} (\ln 2\alpha - 1), \qquad (1.52)$$

and thus, goes to zero essentially as  $1/\alpha^2$ . A graph of D as a function of  $\alpha$ , illustrating that  $0 \le D_x \le 1$ , is shown in Fig. 1.9.

Using the variables illustrated in Fig. 1.8 and the expression for demagnetizing energy in (1.23), it is seen that the demagnetizing energy is given by

$$W_D = \frac{\mu_0}{2} \mathbf{M} \cdot \mathbf{H_D} V = -\frac{\mu_0 M_S^2 V}{2} \left( D_x \cos^2 \theta + \frac{1 - D_x}{2} \sin^2 \theta \right). \tag{1.53}$$

If  $D_x$  is less than 1/3, then  $W_D$  is a minimum when  $\theta = 0$ . If the applied field is now nonzero, then we have to add an applied field energy,  $W_H$ , to this, where according to (1.21),

$$W_H = -\mu_0 \mathbf{H} \cdot \mathbf{M} V = -\mu_0 M_S V [H_x \cos \theta + H_y \sin \theta]. \tag{1.54}$$

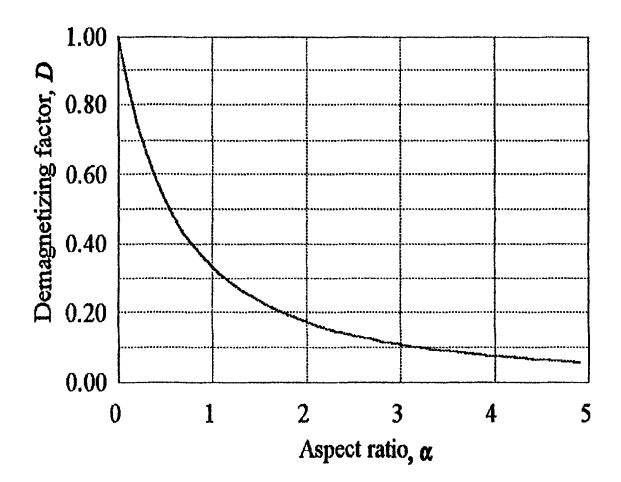


Figure 1.9 The demagnetizing factor of a spheroid as a function of its aspect ratio.

If the body remains uniformly magnetized, then the exchange energy is constant. Since the uniaxial magnetocrystalline anisotropy has the same spatial variation as the demagnetizing field, if their easy axes coincide, the two can be combined into a single term, and the effective demagnetizing factor must be increased by  $K_{n}$ . However, if the long particle axis does not line up with the magnetocrystalline axis, an effective easy axis between the two must be computed. A plot of the total energy, the sum of (1.53) and (1.54), is shown in Fig 1.10, for three applied field values: zero,  $H_k/2$ , and  $H_k$ , where  $H_k = 2K/M$  is called the anisotropy field. It is seen that for zero applied field, the energy has two equal minima 180° apart. Then the magnetization could be oriented along either of these directions. As the field is increased, the minimum near 180° decreases in energy and moves to the left while the minimum near 0° increases and moves to the right. At the critical field, the minimum near 0° disappears, and above that field there is only a single minimum. When the field is decreased back to zero, the energy barrier between the two minima prevents the magnetization from going to the minimum near 0°. Thus, saturating a magnetic material is one method of putting it in a unique magnetic state.

In order to solve for the minimum energy, we take the total energy given by

$$W = -\mu_0 M_S V [H_x \cos \theta + H_y \sin \theta] - \frac{\mu_0 M_S^2 V}{2} \left[ D_x \cos^2 \theta + \frac{1 - D_x}{2} \sin^2 \theta \right], \quad (1.55)$$

differentiate it with respect to  $\theta$ , and set it equal to zero. Thus, after dividing by  $\mu_0$   $M_S V$ , we get

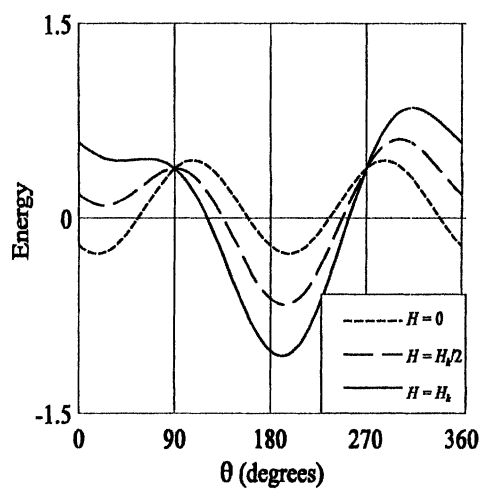


Figure 1.10 Energy as a function of magnetization angle for three applied fields.

$$\frac{1}{\mu_0 M_s V} \frac{\partial W}{\partial \theta} = H_x \sin \theta - H_y \cos \theta - C \sin \theta \cos \theta = 0, \qquad (1.56)$$

where

$$C = M_S \left[ \frac{1 - 3D_x}{2} \right]. \tag{1.57}$$

It is noted that for prolate particles,  $D_x$  is less than 1/3, so that C will be positive. To determine whether this is a minimum or a maximum, we take the second derivative of the energy with respect to  $\theta$ , and obtain

$$\frac{1}{\mu_0 M_s V} \frac{\partial^2 W}{\partial \theta^2} = H_x \cos \theta + H_y \sin \theta + C(\sin^2 \theta - \cos^2 \theta). \tag{1.58}$$

Since the system seeks an energy minimum, this quantity must be positive at a stable equilibrium. To find the critical field,  $H_k$ , that is, the value of the field at which one of the minima disappears, we solve for the value that makes the second derivative zero. Thus, we obtain

$$H_x \cos \theta + H_y \sin \theta + C(\sin^2 \theta - \cos^2 \theta) = 0. \tag{1.59}$$

We can solve for  $\cos\theta$  by multiplying (1.56) by  $\sin\theta$ , multiplying (1.59) by  $\cos\theta$ , and adding the results. Then one obtains

$$\cos \theta = (H/C)^{1/3} \text{ or } H_x = C\cos^3 \theta.$$
 (1.60)

Similarly, we can solve for  $\sin \theta$  by multiplying (1.59) by  $\sin \theta$ , multiplying (1.56) by  $-\cos \theta$ , and adding the results, yielding

$$\sin \theta = -(H_y/C)^{1/3} \text{ or } H_y = -C \sin^3 \theta.$$
 (1.61)

Since  $\sin^2\theta + \cos^2\theta = 1$ , we can eliminate  $\theta$  from (1.60) and (1.61). Thus,

$$H_x^{2/3} + H_y^{2/3} = C^{2/3}$$
. (1.62)

The solution to this equation is called the *Slonczewski asteroid* [9], which is illustrated in Fig. 1.11.

To determine the magnetization and its stability for a Stoner-Wohlfarth particle, one plots the vector magnetic field from the origin, as shown for two field vectors in Fig. 1.11. The direction of the magnetization is obtained by drawing a tangent from the asteroid to the tip of the field vector. The magnetization vector is obtained by drawing a vector whose length is given by  $M_SV$  along that line. It is seen that when  $\mathbf{H_1}$  is applied, the tip of the field vector falls outside the asteroid, and there is a unique state for the magnetization, indicated by  $\mathbf{M_1}$ ; however, when  $\mathbf{H_2}$  is applied, it falls inside the asteroid, and there are two stable states for the magnetization, both of which are indicated by  $\mathbf{M_2}$ .

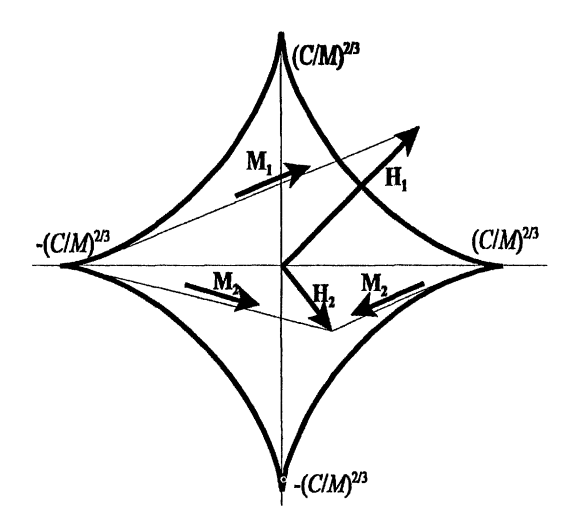


Figure 1.11 Slonczewski asteroid used to determine the state of a Stoner-Wohlfarth particle.

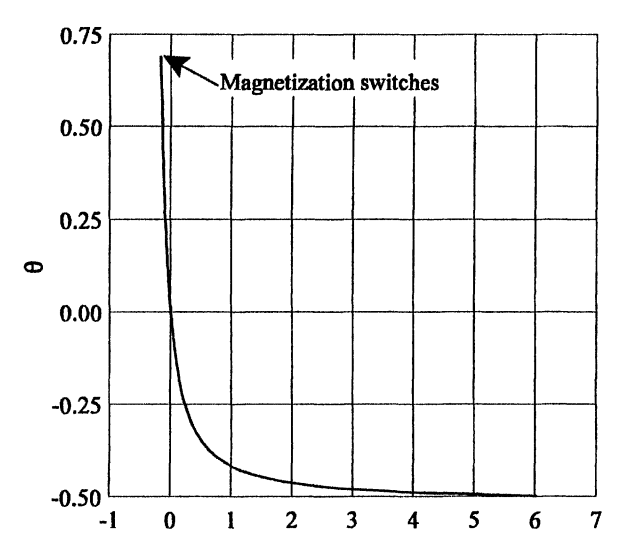


Figure 1.12 Variation of  $\theta$  with the applied field for  $\beta = 0.5$ .

The applied field that achieves this magnetization can be obtained by solving (1.56) as

$$H = \frac{C\sin(2\theta)}{2\sin(\theta + \beta)}.$$
 (1.64)

The variation of  $\theta$  with applied field is illustrated in Fig. 1.12. It is seen that for positive fields,  $\theta$  approaches  $-\beta$  monotonically as the magnetization tries to align itself with the applied field. For negative fields,  $\theta$  increases until it reaches its maximum, and then it switches.

We will define the critical angle  $\theta_M$  as the angle at which the particle switches. It is obtained by solving for the value of  $\theta$  that makes (1.58) equal to zero. It is thus possible to plot m as a function of H by varying  $\theta$  between  $-\beta$  and  $\theta_M$ . That is, one must solve the transcendental equation

$$H\cos(\beta + \theta_{M}) - C\cos(2\theta_{M}) = 0. \tag{1.65}$$

If we substitute (1.64) into this, and use the tangent trigonometric identities, we obtain

$$\tan \theta_{M} = (\tan \beta)^{1/3}. \tag{1.66}$$

If one plotted the component of the magnetization along the applied field's axis, that is,  $M_S \cos(\theta + \beta)$ , as a function of the applied field, one would obtain the hysteresis loops shown in Fig. 1.13 for three values of  $\beta$ . These loops show that for

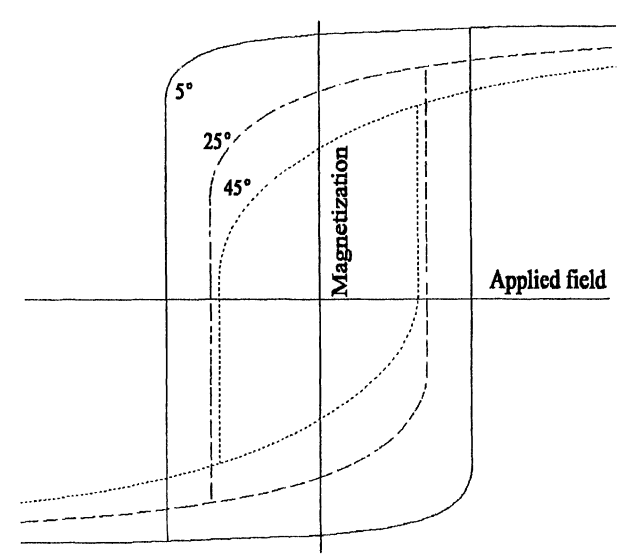


Figure 1.13 Possible Stoner-Wohlfarth particle hysteresis loops for  $\beta = 2^{\circ}$ , 25°, and 45°.

If one plotted the component of the magnetization along the applied field's axis, that is,  $M_s\cos(\theta+\beta)$ , as a function of the applied field, one would obtain the hysteresis loops shown in Fig. 1.13 for three values of  $\beta$ . These loops show that for particles in the negative state, when the applied field reaches the critical field  $H_k$ , the particle abruptly switches to the positive state. If the magnetization was still negative before switching, this field is also the coercivity. On the other hand, if the magnetization was already positive,  $H_k$  is larger than that of the coercivity. The largest value of  $\beta$  for which  $H_k$  is equal to the coercivity is 45°. It is seen that all the hysteresis loops have two critical fields that are the same in magnitude but opposite in sign.

The critical field of a particle as a function of particle angle  $\beta$  with respect to the applied field can then be computed, from (1.62), as

$$H_k = \frac{C}{(\cos \beta^{2/3} + \sin \beta^{2/3})^{3/2}}.$$
 (1.67)

As shown in Fig. 1.14, this field is a maximum when  $\beta = 0$  or  $\pi/2$ . When  $\beta$  increases from 0, the critical field of the particle decreases until  $\beta = \pi/4$ , and then increases back to the value it had at  $\beta = 0$  when  $\beta = \pi/2$ .

For values of  $\beta$  beyond  $\pi/4$ , as the field is increased from negative saturation, the magnetization goes through zero before the magnetization switches. Thus, we have to distinguish between the critical field, the field at which the magnetization switches, and the coercivity, the field at which the magnetization is zero. The coercivity follows the critical field until  $\pi/4$ . Beyond that it obeys (1.64) with  $\theta$  set

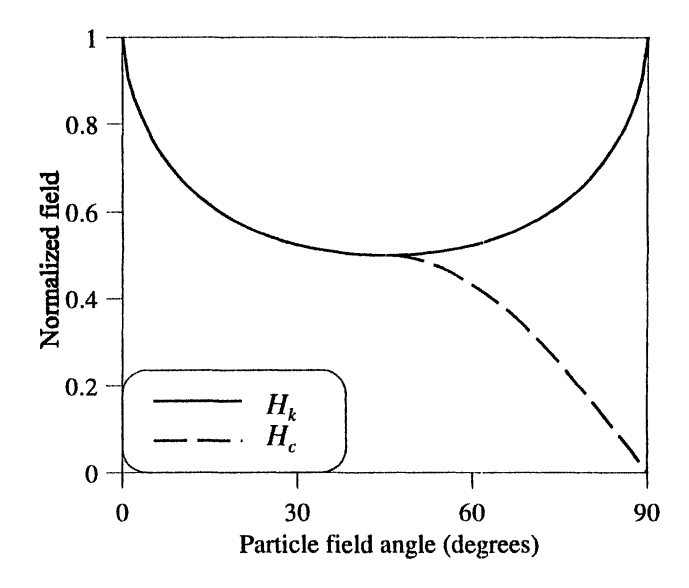


Figure 1.14 Coercivity and critical field variation with particle angle.

to the complement of  $\beta$ , as illustrated in Fig. 1.14. So the field at which the lower section of the curve crosses the H axis is a monotonic decreasing function of  $\beta$ .

For particles that are larger but still single domain, other nonuniform reversal modes are possible. These modes are characterized by smaller values of  $H_C$  and are sometimes referred to as *incoherent reversal modes*. Although these modes have a different  $\beta$  dependence, they have the same properties as the Stoner-Wohlfarth particles: two stable states, a monotonic decreasing function of  $H_C$  with  $\beta$ , and a maximum in  $H_C$  when  $\beta$  is 0 or  $\pi/2$ .

Real particles are generally ellipsoidal but with "corners." These corners permit magnetization reversals to be nucleated with fields considerably smaller than those necessary to nucleate reversals in ellipsoids. Since the shape of the particles prevents the existence of analytical solutions for them, reversal modes of these types have been studied numerically [10,11]. It was seen that for real particles, although their specific properties differ in magnitude and in various details, their general properties are the same as those of Stoner-Wohlfarth particles: that is, they have two stable states for a certain range of particle sizes; their switching field at first decreases with angle and then increases; and their coercivity is a monotonic decreasing function of angle.

One difference between ellipsoidal and nonellipsoidal particles is that for the latter there is a nucleation volume that, once reversed, causes the whole particle to reverse. This is also referred to as the activation volume, and it usually has an aspect ratio of unity. It may be thought of as the largest sphere that can be inscribed within the particle.

# 1.7 MAGNETIZATION DYNAMICS

Hysteresis is a rate-independent phenomenon; that is, the final state is the same no matter how fast the input changes to the final value. In fact, hysteresis is only a function of the field extrema. Thus, to obtain the possible final states, it is necessary only to solve the static equilibrium problem. To choose the particular magnetization pattern that is appropriate for a given input sequence if only hysteresis were involved, one would have to be sure only that the energy, in the sequence of magnetization patterns that were traversed by this magnetizing process, was a monotonically decreasing function of time. Other dynamic effects, which we will now discuss, may alter this sequence of equilibria.

There are two categories of dynamic effects: those that have time constants much slower than the rate of the applied field, and those that are comparable to or faster than the rate of the applied field. The former type includes magnetic aftereffect, which causes the magnetization to drift with time, while the latter type includes eddy currents and gyromagnetic effects. A rate-independent effect sometimes confused with these is accommodation. Accommodation is another process that causes the magnetization to drift; however, this process requires a change in applied field to trigger it. It is observed that repetitive minor loops apparently drift toward an equilibrium loop. As such, it is a rate-independent process and is discussed in Chapter 5.

Aftereffect refers to the slow change in magnetization with time that results from thermal processes. The magnetization is held in an equilibrium pattern by energy potential barriers. They may be surmounted by thermal energy according to the Arrhenius law. When this happens, the magnetization will find another local energy minimum. The higher the potential barrier, the longer it will take to be surmounted, but given enough time, any barrier may be surmounted. With this process, a magnetization pattern will change from a local energy minimum to a global energy minimum. For soft materials, with small energy barriers, this process will take the order of many minutes, but with harder materials, with correspondingly larger energy barriers, it may take centuries. This also is discussed in greater detail in Chapter 5.

# 1.7.1 Gyromagnetic Effects

We now turn our attention to gyromagnetic effects. When a magnetic field is applied to an electron, it creates a torque **T** on its magnetic moment **m** to align it with the magnetic field **B**. That is,

$$\mathbf{T} = \mathbf{m} \times \mathbf{B}. \tag{1.68}$$

Since an electron also has an angular momentum, k, we write

$$\mathbf{m} = -\frac{g\mu_0 e}{2m} \mathbf{k} = -\gamma \mathbf{k}, \tag{1.69}$$

where the minus sign is due to the sign of the charge of the electron, e/m is the ratio of the charge to the mass of an electron, and g is the gyromagnetic ratio, which is one for orbital motion and two for spin motion. The term  $\gamma$  is normally referred to as the gyromagnetic ratio of an electron. Thus, when an electron is subject to an applied magnetic field, its magnetization is unable to align itself with the field, but instead its magnetization precesses about the magnetic field. The precession frequency  $\omega_0$  is given by

$$\omega_0 = \gamma B. \tag{1.70}$$

This rotating magnetic moment radiates energy, thus permitting the electron to eventually align itself with the magnetic field. Therefore, the time rate of change of angular momentum is given by the Landau-Lifshitz equation

$$\frac{d\mathbf{k}}{dt} = -\gamma \mathbf{m} \times \mathbf{B} - \alpha \mathbf{m} \times (\mathbf{m} \times \mathbf{B}), \qquad (1.71)$$

where  $\alpha$  is the damping factor. For small damping factors, the moment will precess many times about the applied field, but for large damping factors, the moment will make a small fraction of a revolution about the applied field as it approaches equilibrium.

When an alternating rf magnetic field with frequency  $\omega$  is applied to a material that is magnetized by a dc field acting along the z-direction, the material appears to have a nonreciprocal permeability tensor given by

$$[\mu] = \mu_0 \begin{bmatrix} 1 + \chi_{xx} & \chi_{xy} & 0 \\ -\chi_{xy} & 1 + \chi_{xx} & 0 \\ 0 & 0 & 1 \end{bmatrix}, \qquad (1.72)$$

where the reciprocal susceptibility is given by

$$\chi_{xx} = \frac{\omega_0 \gamma B}{\omega_0^2 - \omega^2},\tag{1.73}$$

and the nonreciprocal susceptibility is given by

$$\chi_{xy} = \frac{j\omega\gamma B}{\omega_0^2 - \omega^2}.$$
 (1.74)

It is noted that B is the internal field in the material, which in ferromagnetic materials is given by

$$B = \mu_0 M D, \tag{1.75}$$

where D is the demagnetizing factor along the axis on which the material is magnetized. The nonreciprocal nature of this permeability permits one to build nonreciprocal passive devices, such as isolators, circulators, and other similar microwave devices.

# 1.7.2 Eddy Currents

When a field parallel to the magnetization on one side of a domain is applied, the domain wall experiences a "pressure" in a direction that would make the domain parallel to the applied field grow. In conductors, eddy currents are induced by Faraday's law whenever the applied field changes and consequently the magnetization changes. The eddy current field opposes the applied field and generally shields the interior of the material from it. For low frequencies, the applied field eventually penetrates the entire material. For high frequencies, the induced currents and the applied fields are limited to a very thin region close to the surface of the conductor, and so this effect is called the *skin effect*.

# 1.7.3 Wall Mobility

We will now address the question of how a domain wall moves in view of the constraints imposed by the Landau–Lifshitz equation. Consider a  $180^{\circ}$  Bloch wall between two domains magnetized in the +z direction and the -z direction. A z-directed field applies a pressure on the wall tending to move it in a direction such that the domain magnetized in the z direction would grow. This field would not apply a torque on the magnetic moments in either domain, since it has no component perpendicular to the magnetization. The atoms in the wall, however, experience a torque and will start to precess about the applied field. If this continues, the Bloch wall will become a Néel wall and will experience a demagnetizing field perpendicular to the applied field. The magnetic moments in the wall can now precess about this new field, and thus propagate the wall.

The larger the applied field, the faster the atoms in the domain wall will precess, and the more the Bloch wall will convert into a Néel wall. This will produce a larger demagnetizing field in the wall, causing it to precess faster, and thus the wall will move faster. Therefore, the wall's velocity will be proportional to the applied field, and its motion will be characterized by a mobility. This linear variation of wall velocity with the applied field terminates when the wall has completely converted to a Néel wall, and then the wall will have achieved a limiting velocity, referred to as the *Walker velocity*. This velocity depends on the material, but for most materials it is of the order of meters per second. The slowness of this motion was a limiting factor in bubble memories.

## 1.8 CONCLUSIONS

Modeling magnetic materials can be performed at various levels of detail: the atomic level, the micromagnetic level, the domain level, and finally at the nonlinear level. The first of these involves the use of quantum mechanics to compute the magnetization of individual electrons in atoms. The second level smears out the effect of individual atoms into a continuous function, and one can see the variation of the magnetization in the medium on a greater scale. At the domain level, the details of domain walls are invisible, and one sees only uniformly magnetized domains separated by domain walls of zero thickness. Finally, at the nonlinear level, one averages the magnetization over many thousands of atoms in order to replace the constituent equations that complete the definition of magnetic fields along with Maxwell's equation.

Preisach modeling, which we will describe in the subsequent chapters, falls into the nonlinear level of magnetization detail. This type of modeling describes not only gross effects, such as the major hysteresis loop, but also the details of minor loops. When coupled with the appropriate equations, it can describe dynamic effects as well. Finally, it can be coupled with phenomena of other types to describe hysteresis in such effects as magnetostriction.

The solution for the magnetization involves the calculation of the magnetic state of the system, since the behavior depends upon this. Then one can compute the magnetization of the system under the influence of an applied field when the magnetization is in this state. This type of problem is similar to a many-body problem, except that the system displays hysteresis. Thus, it can be referred to it as the *hysteretic many-body* problem.

In modeling coercivity, the quantities of interest are the discrete magnetization states and the Barkhausen jumps that occur when going from one state to another. The minimum change of state is the reversal of a single hysteron or magnetic entity. When there are many interacting hysterons, one is solving a hysteric many-body problem. Then one can go to the limit of a continuous density of hysterons. Preisach modeling is one of the mathematical tools for handling such densities.

The definition of the magnetic state will be based on the Preisach definition of *hysteron*, that is, a region that switches as a single entity and has two magnetic states. For hard materials, this region might be a single particle in particulate media or a single grain in thin-film media; for soft materials, it might be the volume switched by a single Barkhausen jump. A discrete entity with more than two states can be decomposed into several hysterons. Thus, the basic approach is identical for hard and soft materials, but the parameters chosen will differ. The classical Preisach model, which is discussed in the next chapter, is able to describe hysteresis in general, but the details do not accurately describe real-world phenomena. Subsequent chapters modify this model to correct these errors, using the physical principles just discussed.

#### REFERENCES

- [1] A. H. Morrish, *The Physical Principles of Magnetism*, Wiley: New York, 1965.
- [2] S. Chikazumi with S. H. Charap, *Physics of Magnetism*, Wiley: New York, 1964.
- [3] A. Visintin, *Differential Models of Hysteresis*, Springer-Verlag: Berlin, 1994.
- [4] M. Brokate and J. Sprekels, *Hysteresis and Phase Transitions*, Springer-Verlag: New York, 1996.
- [5] F. W. Sears, *Thermodynamics*, Addison-Wesley: Reading, MA, 1959.
- [6] R. Becker and W. Döring, *Ferromagnetismus*, Springer-Verlag: Berlin, 1939.
- [7] E. C. Stoner and E. P. Wohlfarth, "A mechanism of magnetic hysteresis in heterogeneous alloys," *Philos. Trans. R. Soc. London*, **A240**, 1948, pp. 599–642.
- [8] R. M. Bozorth, Ferromagnetism, An IEEE Classic Reissue, IEEE Press: New York, 1994, p. 849.
- [9] J. C. Slonczewski, *IBM Research Memorandum*. No. RM 003.111.224, October 1, 1956.
- [10] M. E. Schabes and H. N. Bertram, "Magnetization processes in ferromagnetic cubes," J. Appl. Phys., 64, August 1988, pp. 1347–1357.
- [11] Y. D. Yan and E. Della Torre, "Modeling of elongated fine ferromagnetic particles," *J. Appl. Phys.*, **66**, July 1989, pp. 320–327.